공학석사 학위논문

Facile synthesis of Au-graphene nanocomposite for the selective determination of dopamine

도파민의 선택적인 검출을 위한 금 나노입자-그래핀 나노 복합재의 간편한 합성

2013년 8월

서울대학교 대학원

나노융합전공

곽 민 정

Facile synthesis of Au-graphene nanocomposite for the selective determination of dopamine

도파민의 선택적인 검출을 위한
금 나노입자-그래핀 나노 복합재의 간편한 합성

지도교수 박 원 철
이 논문을 공학석사 학위논문으로 제출함

2013년 8월

서울대학교 대학원
융합과학부 나노융합전공
곽 민 정

곽민정의 석사 학위논문을 인준함
2013년 8월

위 원 장 김 연 상 (인)

부위원장 박 원 철 (인)

위 원 송 윤 규 (인)

Facile synthesis of Au-graphene nanocomposite for the selective determination of dopamine

Minjeong Kwak

Program in Nano Science and Technology

Department of Transdisciplinary Studies

The Graduate School

Seoul National University

Abstract

In this study, an ultrasensitive electrochemical biosensor for dopamine, which was based on graphene/gold nanocomposite, has been developed. Dopamine (DA) is an important neurotransmitter compound in the mammalian central nervous system because the loss of dopamine containing neurons brings about some serious disease. Therefore, it is very important to develop a selective and sensitive sensor for the analysis of DA in an excess amount of ascorbic acid (AA). Here, we present a facile strategy for the deposition of gold nanoparticles on graphene sheets with high reproducibility. The graphene oxide is synthesized by the modified Hummers method and reduced by chemical and thermal methods after deposition of gold nanoparticles. The graphene/gold nanocomposites were prepared using sodium hydroxide acting as an accelerator for the reduction of gold ions. The possible formation mechanism of graphene/gold nanocomposites without any reducing agent, for example, $NaBH_4$ and sodium citrate etc., was also discussed. The composition and electrochemical properties of the resulting materials were characterized by X-ray diffraction (XRD), X-ray photoelectron spectroscopy (XPS), raman spectroscopy, thermogravimetric analyzer (TGA), cyclic voltammetry (CV) and

differential pulse voltammetry (DPV). Also, transmission electron microscope (TEM) was employed to demonstrate the successful deposition of gold nanoparticles on the surface of graphene sheets. In comparison to the reduced graphene oxide (rGO) modified electrode, the graphene/gold nanocomposite modified electrode shows superior performance. The modified electrode showed a low detection limit (0.208 μM), an enhanced electrocatalystic current for DA, and a good separation of potential of DA and AA.

Keyword : Graphene/Au NPs nanocomposite, Sodium hydroxide, Biosensor, Voltammetric sensing, Dopamine, Ascorbic acid

Student Number : 2011-23982

Contents

List of figures

a to h) on the rGO/Au NPs modified GCE in pH 7.4 PBS at a scan rate of 50 mV · s^{-1} (left) and the calibration curve for DA (right).

Figure 11. CVs (left) and DPVs (right) of 1×10^{-4} M DA on bare GC (solid), rGO modified GC (dot) and rGO/Au NPs modified GC (dash) electrodes in 0.1 M PBS (pH 7.4). Scan rate : 50 mV s^{-1}.

Figure 12. CVs (left) and DPVs (right) of a mixture 1×10^{-4} M DA + 1×10^{-3} M AA at bare GC (solid), rGO modified GC (dot) and rGO/Au NPs modified GC (dash) electrodes. Electrolyte : 0.1 M PBS (pH 7.4). Scan rate : 50 mV s^{-1}

1. Introduction

Nanoscience is the term used to describe the research and development of materials have at least one dimension in the nanometer range. Now days, nanotechnologies and nanoscience, which have become one of the most rapidly growing field of research, which sit at the point of convergence of several disciplines (physics, chemistry, biology, mechanics, etc.) [1]. Nanoscale materials have very high surface to volume ratio, many potentials for use in composite materials, reacting systems, drug delivery and chemical energy storage (such as hydrogen and natural gas) [2]. Electroanalytical chemistry is a rising convergence technology field, which integrates with characteristics of electrochemistry (e.g., rapid detection speed, low detection limits, small size, rapid, low price, and compatibility with microfabrication technology) with unique properties of nanomaterials (e.g., electronic, optical, magnetic, mechanical, and catalytic) to become one of the most interesting topics. [3]

1.1 Dopamine and ascorbic acid

Dopamine (DA) is one of the most important neurotransmitters playing a significant role in central nervous, renal and hormonal systems [4,5]. As a chemical messenger, dopamine is similar to

adrenaline. Dopamine affects brain processes that control movement, emotional response, and ability to experience pleasure and pain [6,7]. DA is found in humans as well as animals, including both vertebrates and invertebrates. DA is also used as medication and acts on the sympathetic nervous system. Application of DA leads to increased heart rate and blood pressure. DA cannot cross the blood-brain barrier, so it given as a drug does not directly affect the central nervous system [8]. Dopamine is needed in some brain diseases as well. This includes diseases such as Parkinson's disease and dopa-responsive dystonia. For these patients levodopa which is a precursor of DA is used and can cross the blood-brain barrier [9].

Ascorbic acid (vitamin C) is as essential to plants as it is to animals. Ascorbic acid (AA) functions as a major redox buffer and as a cofactor for enzymes involved in regulating photosynthesis, hormone biosynthesis, and regenerating other antioxidants. AA is a water-soluble antioxidant that serves a predominantly protective role. Despite the fact that most mammals can synthesize ascorbate (Asc), humans (along with other primates, bats, and guinea pigs) are unable to make vitamin C as a result of a mutation to the gene encoding L-gulono-1,4-lactone oxidase, the last enzyme in the Asc biosynthetic pathway [10].

The detection of DA by electrochemical methods has received

considerable interest because of its good eletrochemical activity. However, The very low concentration of DA in the "extracellular fluid" of the caudate nucleus requires sensitive detection methods for DA. It also coexists with excess AA in real biological sample and both are electroactive materials (Figure. 1). So it is quit hard to analyze DA with high selectivity [11,12]. Since the concentration of AA is about 1000 times higher than DA, the direct oxidation of AA at the electrodes occurs at a similar potential so that overlap that of DA [13]. Therefore, the diagnostic tool that is capable of selective detection of DA in the excess AA is demanded. Many attempts have been made on the development of highly selective dopamine biosensor but still need more investigations [14-17]. Herein we suggest a sensitive dopamine biosensor using a rGO/Au NPs nanocomposite modified GCE which shows good selectivity for DA in the presence of high concentration of AA.

1.2 Cyclic voltammetry

Cyclic Voltammetry (CV) is an electrochemical technique which measures the current that develops in an electrochemical cell under conditions where voltage is in excess of that predicted by the Nernst equation [18]. CV is performed by cycling the potential of a working electrode, and measuring the resulting current. CV has become a

popular technique for electrochemical studies. The system consists of an electrolysis cell, a potentiostat, a current-to-voltage converter, and a data acquisition system. The electrolysis cell consists of a working electrode, counter electrode, reference electrode, and electrolytic solution. The counter electrode simply conducts electricity through the solution from the signal source to the working electrode. The role of the electrolytic solution is providing ions to the electrodes during redox reaction. The current-to-voltage converter measures the resulting current, and the data acquisition system produces the resulting voltammogram. CV has been believed to good for researching about complex electrode reactions, electrode reaction kinetics, and electrode physical condition. CV can be employed to investigate qualitative information about electrochemical processes under various conditions, such as the presence of intermediates in oxidation-reduction reactions, the reversibility of a reaction as well. In addition, since concentration is proportional to current in a reversible, the concentration of an unknown solution can be determined by generating a calibration curve of current vs. concentration [19]. In this study, CV was employed for DA analytes, especially selectivity of detection. In addition, we observe some physical characterization of the rGO/Au NPs modified electrode.

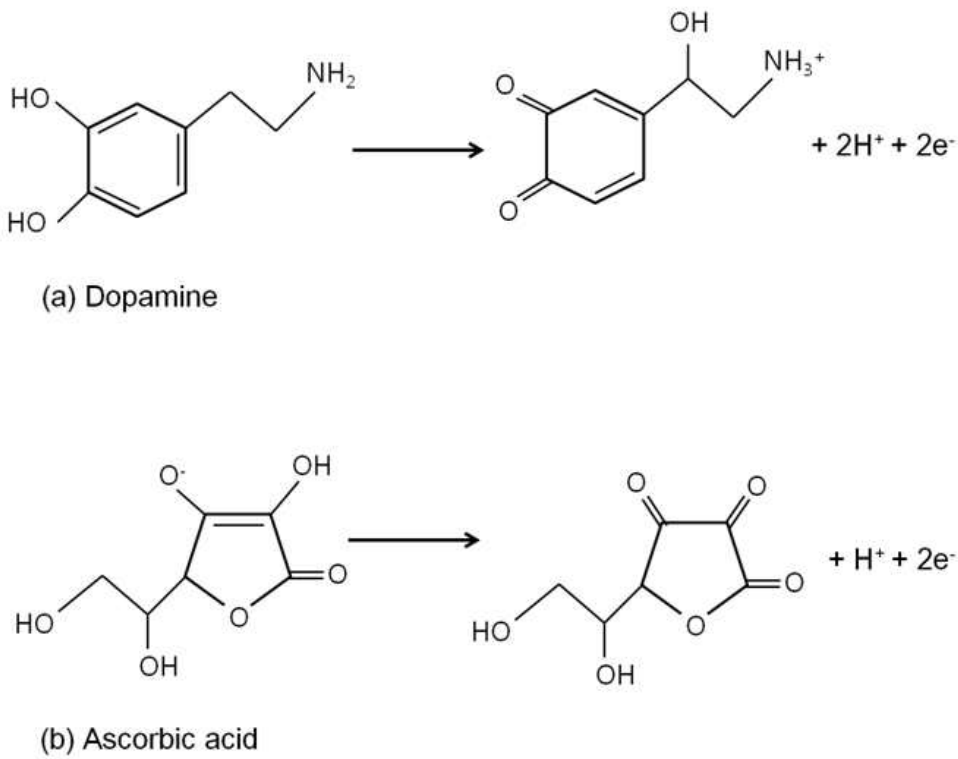

Figure. 1 Mechanisms of (a) DA and (b) AA electrochemical oxidation

1.3 Graphene

Carbon nanomaterials including carbon nanotubes (CNTs) [20-22], carbon nanofibers [23], and highly ordered mesoporous carbon (OMCs) [24] etc. are most widely used in electroanalysis and electrocatalysis since they have great potentials for constructing electrochemical sensing platforms, high sensitivity to detect different target molecules and relatively high chemical stability [25-30].

Graphene, a single layer graphite with close-packed conjugated honeycomb lattices, has especially attracted tremendous attention from scientific communities since the experimental observation of single layers by K. S. Novoselov and A. K. Geim in 2004 [31,32]. Graphene has the excellent mechanical strength, and chemical stability. Moreover, it posses remarkably high charge mobility under ambient conditions with reported values in excess of 15000 $cm^2/(V\ s)$ [33,34]. It is recognized as the basic building block of all-dimensional graphitic materials and one of the lightest, strongest and most conductive materials ever known. It provides a variety of novel applications such as field-effect transistor (FETs) [35], energy storage [36], biotechnologies [37], transparent electrodes [38] and novel nanocomposites [39]. Above all, graphene possess excellent merits in biosensing due to its biocompatibility, large detection area and high electron mobility [40]. Considering the

wide-ranging potential applications of a two-dimensional graphene sheet as a host material for a variety of nanoparticles, many research works have been made for the fabrication of hybrid nanoparticle–graphene structures endowed with multiple functionalities.

Graphene oxide (GO) is prepared by an acid treatment of graphite. GO is a promising precursor for preparing graphene-based composites and electronics applications. Moreover, the oxygen groups that are attached with covalent bond including epoxy, hydroxyl and carboxylic groups are not only advantageous for electrochemical applications also effectively used to produce graphene-based composite materials [41]. Graphene-based composite materials prepared via molecular-level dispersion in polymers have shown to improve electronic and thermal conductivity [42]. The extraordinary properties of graphene-based composite materials may provide insight to fabricate novel biosensors for virtual applications. The high surface area of graphene is helpful in increasing the surface loading of the target molecules and catalytic metal nanoparticles on the surface. The excellent conductivity and small band gap are favorable for conducting electrons from the biomolecules [41]. Graphene-based composite biosensors can also have a much higher sensitivity because of the low electronic noise from thermal effect [43].

Nanomaterials made of noble metals like Au, Ag, Cu, Pt, and Pd are being widely studied for various applications. These nanomaterials are found to have potential applications in various fields like sensor technology [44], optical devices [45], catalysis [46], biological labeling [47], drug delivery system [48], and treatment of some cancers [49]. Attempts have been made in the past decade or so to assemble metallic particles of various shapes and obtain well-organized nanostructures. These noble metal nanoparticles exhibit new physico-chemical properties which are not observed either in the individual molecules or in the bulk metals [50].

Among them, gold nanoparticles (Au NPs) have attracted much attention owing to their large surface area, superior electronic conductivities, and great catalytic properties. Au NPs have been considered to have potential in biological and medical field. Despite the fact that gold is a poor catalyst in bulk form, nano-sized Au NPs exhibit unique advantages such as catalytic activity, enhancement off mass transport and interface-dominated properties [51]. Due to these special properties of Au NPs, great research interests have been attracted to fabricate electrochemical sensors and biosensors. In addition, it is also demonstrated that Au NPs could be used to construct interfaces for the electrocatalysis of oxidation and reduction of many

important biomaterials [52].

The dispersion of Au NPs on graphene sheets potentially provides a new way to develop catalytic and optoelectronic materials. Recently, various methods have been reported to synthesis Au-graphene hybrids. Several studies have been reported on the construction of electrochemical biosensors using Au/graphene composite nanomaterials [53-55].

In this work, we demonstrate a simple approach to prepare GO/Au NPs nanocomposite. GO/Au NPs was then reduced throughly by chemical and thermal processes to prepare Au/reduced graphene oxide (rGO/Au NPs). This approach has two advantages. (1) Au NPs were grown directly on GO sheets without capping agents or surfactants. (2) The surface of GO sheets has many defects and abundance of functional groups (such as carboxyl, carbonyl, hydroxyl and epoxide) so that Au NPs were uniformly deposited on GO rather than on rGO which has less functional groups. Au NPs are reduced separately or partially decorated on rGO.

The glassy carbon electrode (GCE) was modified with rGO/Au NPs film to develop a novel electrochemical sensor for the detection of DA in the presence of AA. The modified electrode exhibited high electrocatalytic activities toward oxidation of DA and AA, and displayed

good voltammetric peak separation between DA and AA. The preparation and electrochemical behavior of the modified electrode were investigated in detail.

2. Experimental

2.1. Reagents and materials

Graphite powder (<20 μm), hydrazine, ammonia, N,N-dimethylformamide (DMF), H_2SO_4, $KMnO_4$, 0.01 M phosphate buffered saline (PBS; 0.138 M NaCl, 0.0027 M KCl, pH 7.4), sodium hydroxide, dopamine hydrochloride (DA) and L-ascorbic acid (AA) were purchased form Aldrich and used as received. Doubly distilled water was used throughout the whole experiments. Dopamine hydrochloride and L-ascorbic acid solutions were freshly prepared in PBS prior to use.

2.2. Instruments and measurements

The electrochemical measurements were conducted with an AUTO-LAB potentiostat (Metrohm, USA) using a conventional 3-electrode system. The electrochemical cell consisted of glassy carbon electrode (GCE, 3 mm diameter, Bioanalytical Systems, Inc.) as the working electrode, Ag/AgCl (Bioanalytical Systems, Inc.) as the reference electrode, and platinum wire as the counter electrode. The sweep rate in the CV measurement was 50 mV s^{-1}.

X-ray diffraction (XRD) pattern of the as-synthesized rGO/Au NPs nanocomposite was obtained from Bruker D-5005 with Cu Kα radiation (λ = 1.5406 A) at 40 kV and 40 mA. Transmission electron microscopic (TEM) observations were made on a JEOL EM-2010 microscope at an accelerating voltage of 200 kV and a JEM-3010 (JEOL) at an accelerating voltage of 300 kV. Raman spectra was obtained using Dongwoo DM500i Raman microprobe with a 15 mW Argon laser at 514.5 nm excitation. The composition of each component within the rGO/Au NPs nanocomposite was measured using a thermogravimetric analyzer (TGA, Mettler-Toledo TGA)

2.3. Synthesis of graphene oxide

Graphene oxide (GO) powders were synthesized from oxidation of graphite according to the modified Hummer's method [56,57]. Typically, 72 mL of 95% H_2SO_4 and 8 mL of 85% H_3PO_4 were added into 500 mL beaker filled with 3 g of graphite powder. To avoid rapid heat evolution, 18 g $KMnO_4$ was slowly added. The mixed slurry was stirred mildly at 60 ℃ for 1 h under ice-cooling. The ice bath was removed and the temperature of the suspension was increased to 90 ℃ and maintained at that temperature for 24 hr. After cooling down, 350 mL of deionized water was slowly added into the reacted slurry and

stirred for 2 hr. The reaction was finished by adding 5 mL of 30% hydrogen peroxide solution (H_2O_2). The suspension was separated by centrifugation, washed with 2 M HCl solution. The obtained sample was repeatedly washed with deionized water and followed by ultrasonic treatment for 60 min. The solid product was separated by centrifugation and then dried in a vacuum oven at 60 ℃ for 24 hr.

2.4. Synthesis of rGO/Au NPs nanocomposite

The process of GO/Au NPs nanocomposite preparation is outlined in Figure 2. The GO suspension was prepared by dispersing 0.25 g of GO powder in 250 mL of DI water. After it showed the well-dispersed status of GO in water without any aggregation, 50 mL of 0.01 M $HAuCl_4$ and 37.5 mL of 0.1 M NaOH were sequentially added at room temperature under vigorous stirring for 12 hr. The resultant nanocomposite was isolated by centrifugation (15000 rpm) and resuspended in 87 mL of water to remove residual gold precursor and NaOH. Hydrazine (75 μL) was then added and heated in an oil bath at 80 ℃ with vigorous stirring for 12 hr over which the reduced GO/Au NPs nanocomposite were gradually precipitated out. This product was filtered and dried in a vacuum oven. After that, hydrazine-reduced GO/Au NPs nanocomposite powder was heated and the resulting

material was dried in a vacuum oven for 3 hr. Since the quality of graphene can be improved by thermal treatment, The hydrazine-reduced GO/Au NPs nanocomposite powder was placed into a furnace tube under reducing atmosphere (20% H_2-80% N_2 mixed gas). The temperature was then raised to 300 ℃ and maintained at that temperature for 1 hr. Here after, this material will be referred as thermally reduced GO/Au nanocomposite (rGO/Au NPs).

2.5. Preparation of rGO/Au NPs modified GCE

The GCE was polished successively using 0.3 μm and 0.05 μm alumina powder and rinsed thoroughly with ethanol and deionized distilled water each for 10 min and dried in air before use. rGO/Au NPs nanocomposite powder was dispersed in DMF solvent at a concentration of 0.1 mg mL^{-1} and sonicated until the suspension is homogeneous. A 4 μL of the suspension was then pipetted onto the pretreated GCE surface and dried in air.

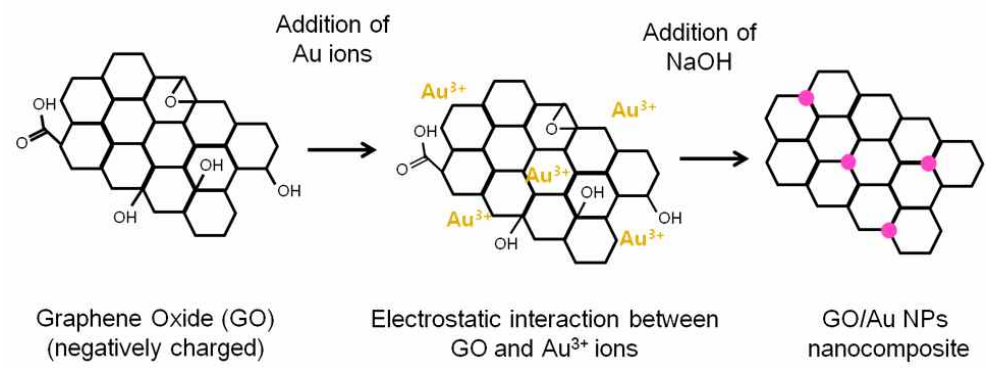

Figure 2. Schematic procedure for the fabrication of GO/Au NPs nanocomposite.

3. Result and Discussion

Study on the formation of rGO/Au NPs

There are two key factors for the formation of Au NPs on GO. First, GO which is prepared from graphite by chemical oxidation has abundant structural defects and oxygen functional groups on the surface, which can be used as anchoring sites for metal nanoparticles [58]. Much quantity of the oxygenated groups on GO sheet will act as an electron-donating source to reduce Au ions and the nucleation of Au NPs occurs spontaneously. It is well known that specific metal ion pairs are oxidized and the other reduced spontaneously in solution. For example, when Zn is exposed to a Cu^{2+} ion in solution, Zn is oxidized and Cu^{2+} is reduced. This reaction takes place spontaneously. In the redox of Zn and Cu^{2+}, electrons flow from each Zn atom to each Cu^{2+} ion. The GO/Au^{3+} system is similar to this Zn-Cu^{2+} redox pair. Oxidative CNT is found that it has the slightly increased work function compared with CNT [59]. Thus, the work function of GO would be slightly higher than that of rGO. The work function of rGO has been found to be 4.88 eV and reduction potential is determined to be +0.38 V vs. SHE (standard hydrogen electrode) [60]. The reduction potential of GO might be around +0.38 V or little bit above, which is still much lower than that of the $AuCl_4^-$ redox pair (+1.002 V vs SHE) [61]. Since the relative

position of reduction potentials between GO and Au ion, reduction of Au ion can be occurred spontaneously.

On the other hand, in this process, NaOH acts as an accelerator for the nucleation of Au NPs without adding additional reducing agent. After the addition of NaOH to the mixture solution of GO and $HAuCl_4$, the solution color was changed from brownish yellow to dark black in a few minutes, which implied the formation of Au NPs [62]. It is well known that the products of $HAuCl_4$ hydrolysis is pH-dependent. Below pH 4, $AuCl_4^-$ is dominant and the concentration of $[AuCl_x(OH)_{4-x}]^-$ increases from pH 5 to 6. At pH 7, $[AuCl(OH)_3]^-$ is prevalent which is more difficult to be reduced than $AuCl_4^-$ and $[AuCl_x(OH)_{4-x}]^-$ [63,64]. The nucleation and growth of Au NPs proceed rapidly, facilitating the formation of well-dispersed fine Au NPs when $[AuCl_x(OH)_{4-x}]^-$ is dominant [65]. Therefore, keeping pH of the reaction solution between 4 and 5 is the key factor to control the nucleation and dispersion of Au NPs.

3.1 Characterization of rGO/Au NPs nanocomposite

Optimization of decorating Au NPs on graphene sheets

The TEM images of the whole synthesis procedure are shown in

Figure. 3. Figure. 3A clearly shows the flake-like shapes of GO nanosheets. The larger size of Au NPs in Figure. 3C is due to reduction of excess gold precursor by hydrazine during the reducing process. Furthermore, we tried to decorate GO with gold nanoparticles more densely by varying the concentration of gold precursor and the reaction time. In the case of varying the reaction time, there are no significant changes in size and density between 1 hr and 5 hr (Figure. 4). Likewise, in this reaction, increasing reaction time which is helpful to formate gold nanoparticles throughly while 5 hr is enough for complete reaction. Figure. 5 shows the dependency of the concentration of gold precursor. We expected that gold nanoparticles would be decorated more densely with higher concentration of gold precursor. However, as concentration of gold precursor is increased, the Au NPs tend to be more agglomerated together. The experimental result indicates that 0.8 of gold precursor/GO concentration ratio is the most suitable and desirable condition for high-yield synthesis of GO/Au NPs nanocomposites. After chemical reduction through refluxing with hydrazine and thermal reduction, GO were reduced to rGO.

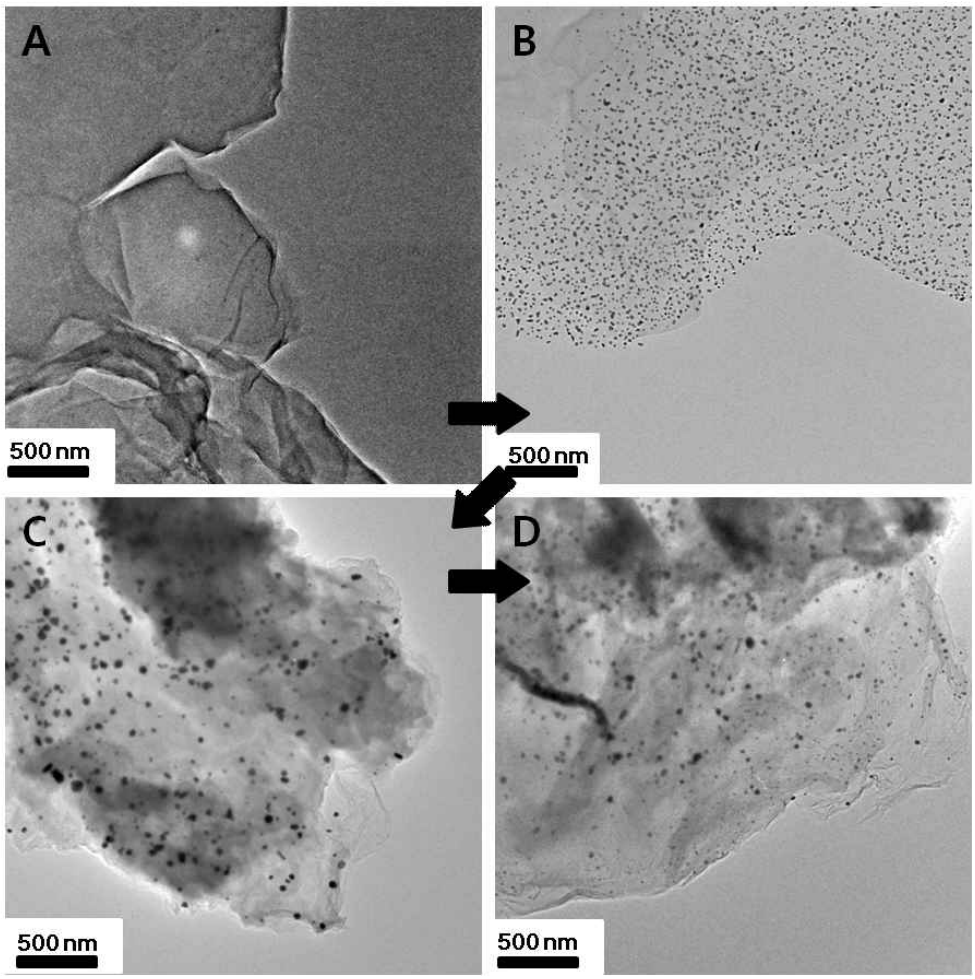

Figure. 3 TEM images of GO (A), GO/Au NPs (B), chemically reduced GO/Au NPs (C) and chemically and thermally reduced GO/Au NPs nanocomposite (D).

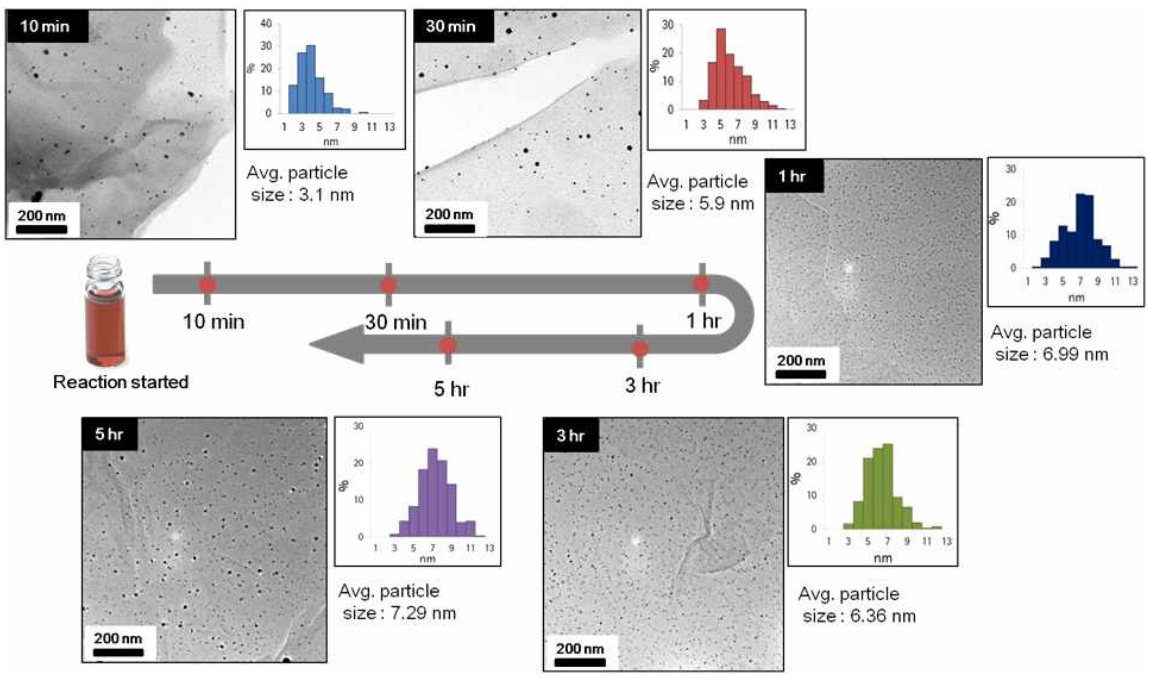

Figure. 4 TEM images and size histograms of GO/Au NPs nanocomposites with different reaction times of 10 min, 30 min, 1 hr, 3 hr and 5 hr after injection of gold precursor respectively.

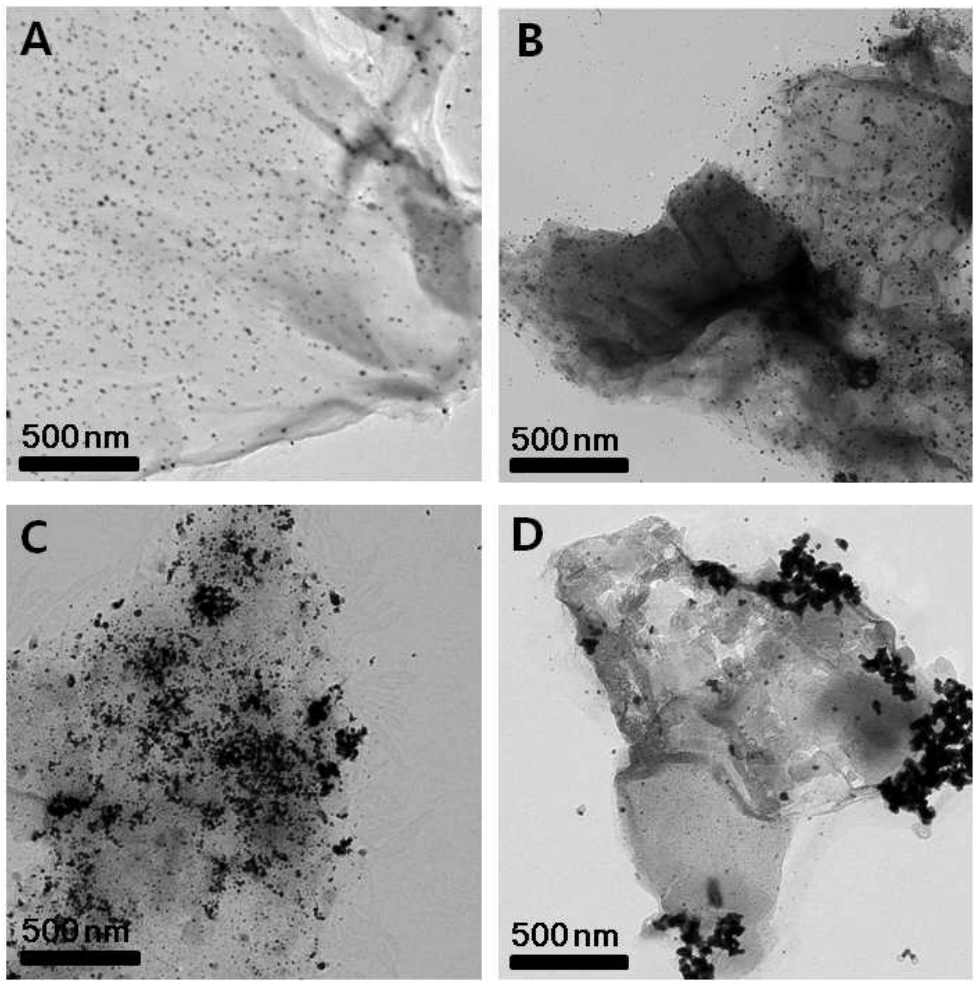

Figure. 5 TEM images of GO/Au NPs with various concentration ratios of gold precursor/GO. The gold precursor/GO concentration ratio is 0.8 (A), 1.6 (B), 3.2 (C) and 4.8 (D) respectively.

The as-synthesized GO/Au NPs nanocomposite was also well characterized by XRD and TGA (Figure. 6). XRD pattern of the GO/Au NPs includes five sharp diffraction peaks at scattering angles of 38.28° , 44.48° , 64.6° , 77.44° and 81.58° corresponding to crystal planes (111), (200), (220), (311) and (222) of gold face-centered cubic crystallographic structure (JCPDS card No. 65-2870). The characteristic peak of GO at 11.3° is also shown in the spectrum [66], so the XRD pattern further indicates that the synthesis of GO/Au NPs nanocomposites is successful. TGA was applied for investigation of the thermal properties of samples. Shown as Figure. 6 (right), TGA curves of GO (a) and rGO/Au NPs (b). GO is thermally unstable and starts to lose weight upon heating. It shows a continuing weight loss of about 20 % in the temperature range up to 188 ℃ and the major mass loss occurs at ~ 200 ℃. However, the TGA curve of rGO/Au NPs decreases slowly until at 150 ℃ and sharply decreases at 150~180 ℃. There was no more major weight loss after that, indicating most of graphene decomposed and only gold metal nanoparticles are left.

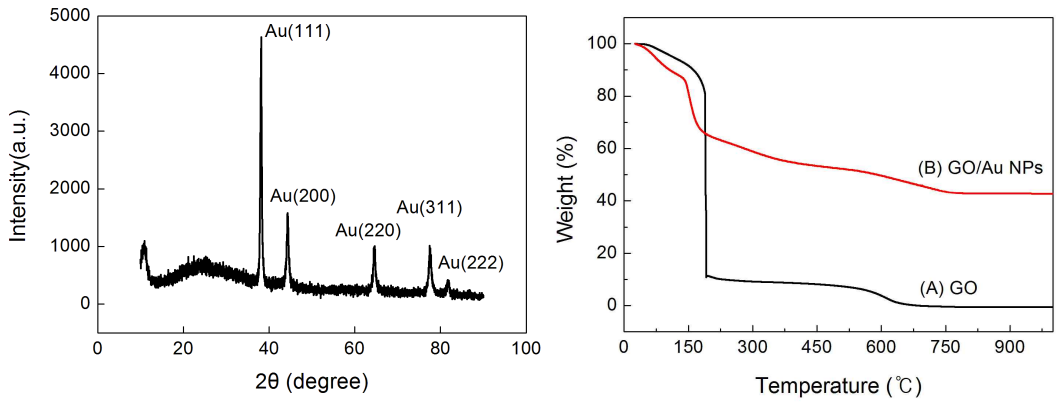

Figure. 6 XRD patterns of the as-synthesized GO/Au NPs (left) and TGA curves of GO (a) and rGO/Au NPs (b). The thermograms were obtained at a scan rate of 10 ℃ min^{-1} under air (right).

The Reducing process of graphene

We have employed X-ray photoelectron spectroscopy (XPS) to analyze the change in the GO component during the reaction (Figure. 7). The relative intensity of the peaks associated with C-C bonds (284 eV) and C-O bonds (286 eV) significantly changed after the chemical and thermal reducing processes compared with the original GO (Figure. 8A). The structural changes are also observable in their Raman spectra (Figure. 8). The Raman spectrums of the as-prepared GO (Figure 8-a) and rGO/Au NPs (Figure. 8-b) display two prominent peaks at 1340 and 1600 cm^{-1}. The intensity ratio of the D and G band is a measure of the disorder, as expressed by the sp^2/sp^3 carbon ratio. As shown in Figure. 9-(B) with the reduction, the ratio of D/G increased significantly. The nucleation and growth of Au NPs may be able to reduce the defects of GO, because the reduction of Au NPs usually occurs at defect sites which is rich with reactivity [67]. This observation also suggests that most of the oxygenated groups are removed by excess hydrazine and thermal process.

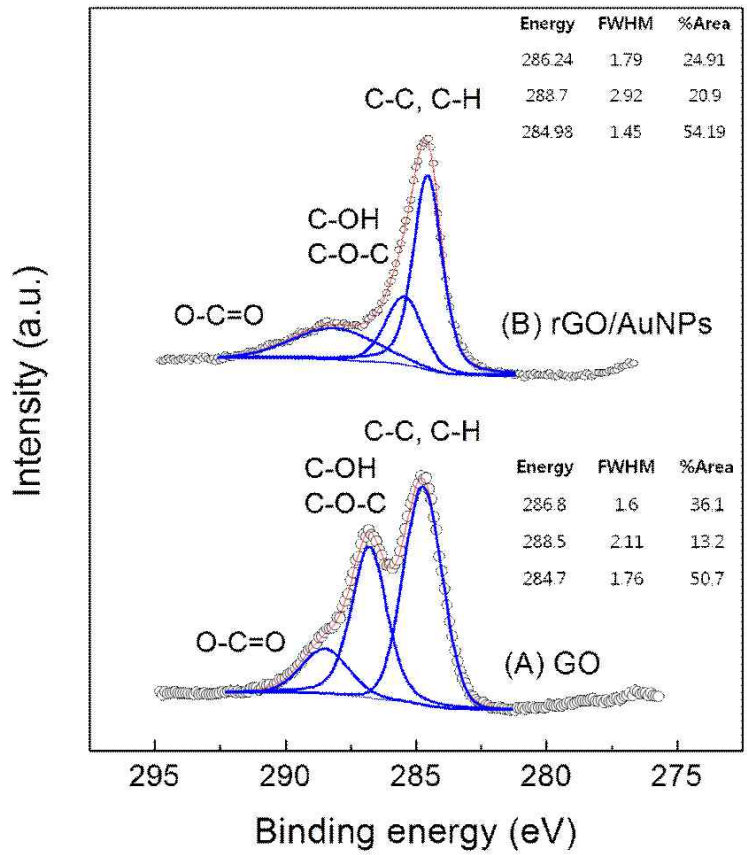

Figure. 7 The C_{1s} XPS spectra of (A) GO and (B) rGO/Au NPs.

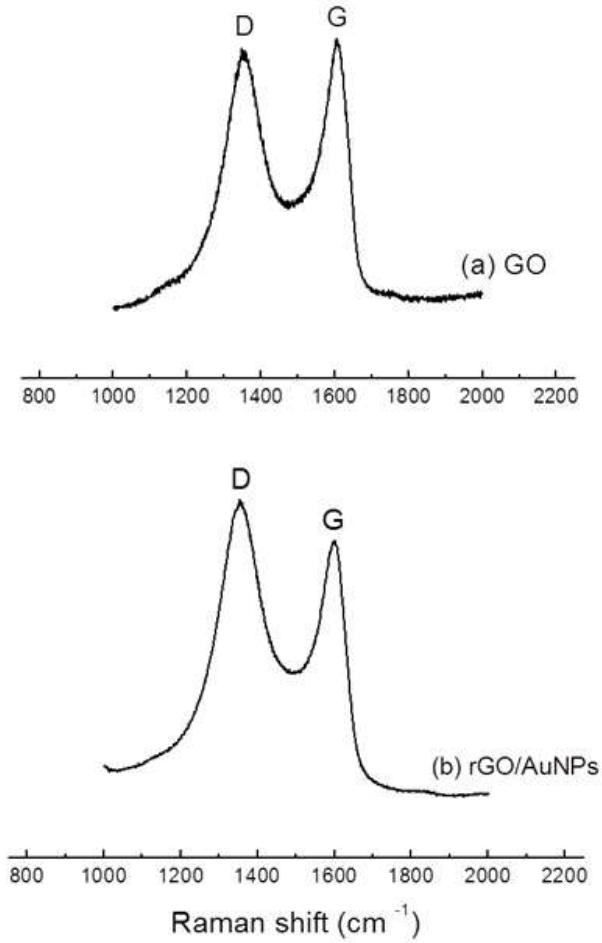

Figure. 8 The Raman spectra of GO (a) and rGO/Au NPs (b).

3.2 Selective determination of DA

Effect of scan rate and concentration of DA

The cyclic voltammetry (CV) curves for 1×10^{-4} M DA was carried out at different scan rates (Figure 9). The peak currents for the anodic oxidation of 0.1 mM DA in 0.1 M PBS (pH 7.4). The plots of anodic and cathodic peak (Figure. 9) show a linear relationship between the anodic (i_{pa}) and cathodic peak current (i_{pc}) in the scan rate (ν) in the range of 20-150 mV s^{-1}. When scan rate is increasing, the E_{pa} moved to positive direction and the both peak currents are elevated, suggesting that the electrochemical kinetics of DA at rGO/Au NPs modified GCE is a quasi-reversible [68].

Figure. 10 shows CV responses of different concentration DA on the rGO/Au NPs modified GCE. The results suggested that i_{pa} was proportional to DA concentration over the range of 1.0×10^{-5} mol L^{-1} to 8.0×10^{-4} mol L^{-1} and obeyed a following equation :

$$i_{pa} = 0.0598\ \mu A\ L\ mol^{-1} \times [DA] + 24.56$$

with the correlation coefficient of 0.9968 (n=10). The standard deviation of peak currents a $\pm 4.146 \times 10^{-9}$ μA. The detection limit of this method is 0.208 μM (S/N=3) under the optimized conditions which is lower than those of graphene-based electrochemical biosensors [17,69].

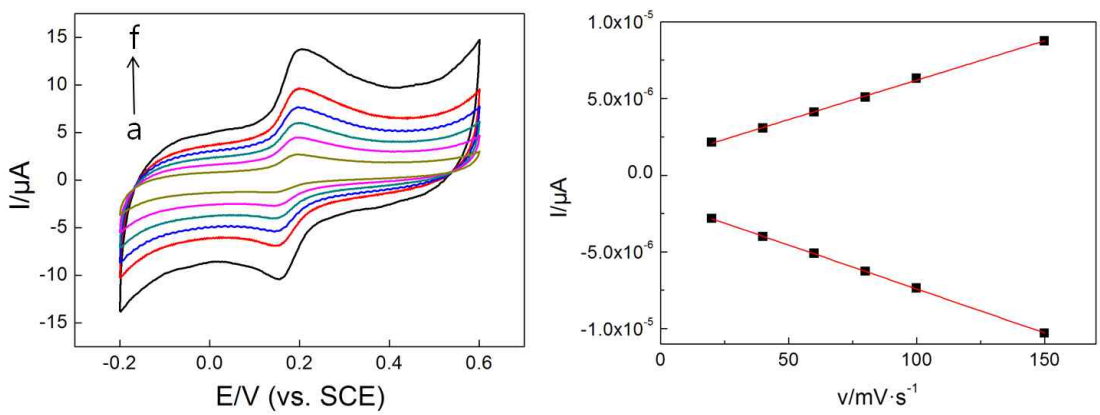

Figure. 9 Effect of scan rate on the voltammograms of the rGO/Au NPs modified GCE in pH 7.4 PBS containing 0.1 mM DA (left) and plots of anodic and cathodic peak current vs. scan rate (right). Scan rate : 20, 40, 60, 80, 100 and 150 $mV \cdot s^{-1}$ (from a to f)

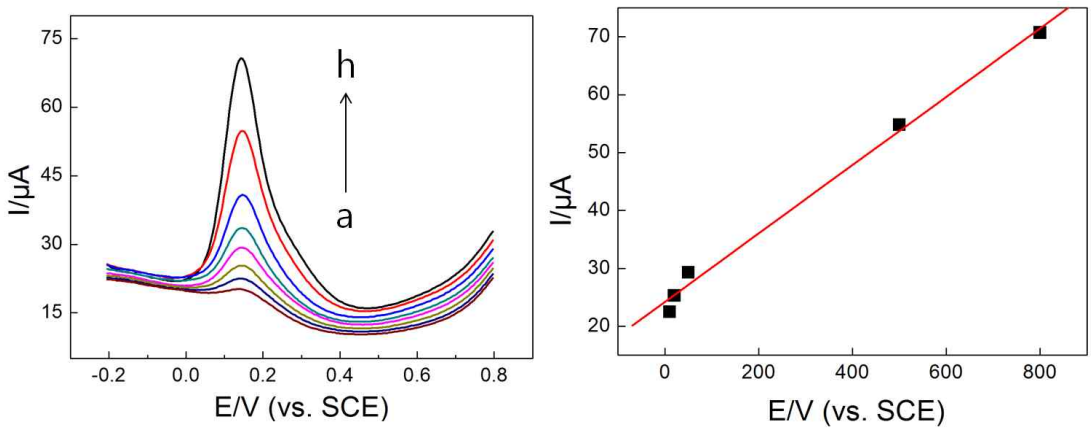

Figure. 10 DPVs of 5, 10, 20, 50, 100, 200, 500 and 800 μM DA (from a to h) on the rGO/Au NPs modified GCE in pH 7.4 PBS at a scan rate of 50 mV · s^{-1} (left) and the calibration curve for DA (right).

Voltammetry behaviors of DA and AA at different electrodes

The response of the different modified electrode in same concentration of DA was shown in Figure. 11. It shows that the anodic peak current (i_{pa}) of DA at rGO/Au NPs modified GCE is about 3.5 times higher than its at the bare GCE. The redox peak currents of rGO/Au NPs modified GCE are also the largest compare to other electrodes, which are about 2 times higher than those at the rGO modified GCE. The large surface area, high conductivity and excellent catalytic activity of graphene and gold nanopartices may be account for the above results.

Since the concentration of AA is much higher than DA, AA causes the strong interference in electrochemical detection of DA. CVs and DPVs of the mixture (1×10^{-4} M DA + 1×10^{-3} M AA) at different electrodes are shown in Figure. 12. As observed in CV and DPV peaks of bare GCE, bare GCE was not able to separate the mixed voltammetric signals and the oxidation peaks were indistinguishable. At the rGO modified GCE, two separate voltammetric peaks are obtained but still not good at displaying peak separation between DA and AA. However, the rGO/Au NPs modified GCE shows two well-defined peaks with significantly enhanced peaks currents. In DPVs, peak separation of rGO/Au NPs GCE is 175 mV, which is larger than its at the rGO

modified GCE (135 mV). From these results, it is proved that the selectivity and sensitivity of rGO/Au NPs modified GCE for DA in the presence of high concentration of AA are enhanced compared to rGO modified GCE, which means the rGO/Au NPs nanocomposite is very good electrode material for electrochemical sensing.

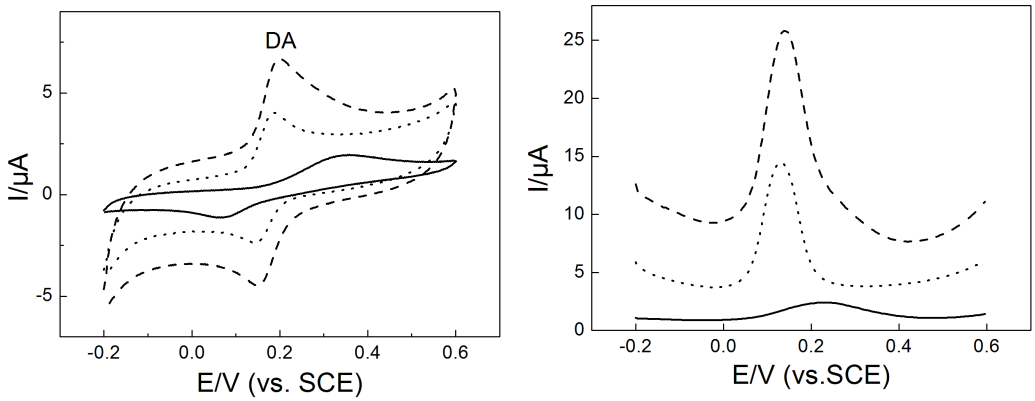

Figure. 11 CVs (left) and DPVs (right) of 1×10^{-4} M DA on bare GC (solid), rGO modified GC (dot) and rGO/Au NPs modified GC (dash) electrodes in 0.1 M PBS (pH 7.4). Scan rate : 50 mV s^{-1}.

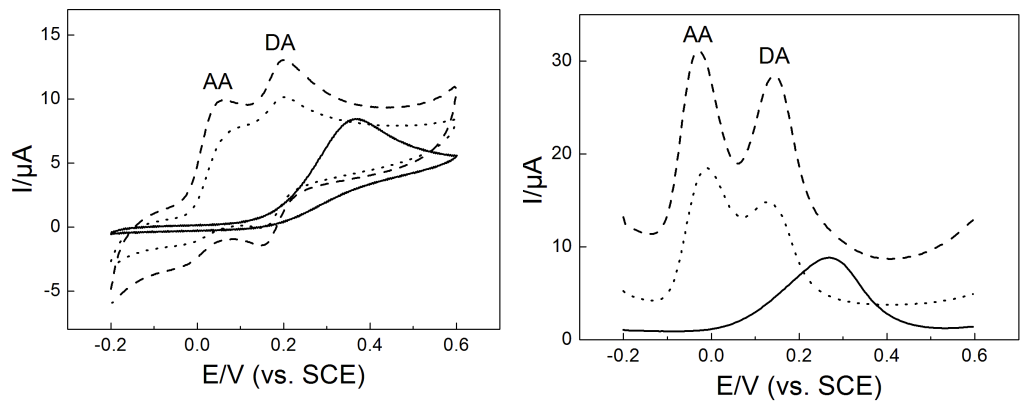

Figure. 12 CVs (left) and DPVs (right) of a mixture 1×10^{-4} M DA + 1×10^{-3} M AA at bare GC (solid), rGO modified GC (dot) and rGO/Au NPs modified GC (dash) electrodes. Electrolyte : 0.1 M PBS (pH 7.4). Scan rate : 50 mV s^{-1}.

Conclusion

In this study, a sensitive electrochemical method for the detection of DA in presence of high concentration of AA is proposed. We have demonstrated a facile and simple method for the fabrication of rGO/Au NPs nanocomposite. The gold nanoparticles are reduced directly on graphene sheets and showed good reproducibility without any reducing agent and heating process. The rGO/Au NPs modified electrode showed significantly enhanced redox peak currents of DA and also resulted in a favorable voltammetric resolution of DA and AA due to high catalytic activity and conductivity of rGO/Au NPs hybrid materials. The observed detection limit for DA is 0.208 μM under the optimized condition which means that it has excellent sensitivity for DA or other electroactive biomolecules. Thus, the developed method demonstrated great potential for detecting DA in pharmaceutical products and real human sample. Furthermore, this novel material may be used for electroanalytical applications such as food or environment monitoring.

References

[1] Murday, J. S., *AMPTIAC Newsletter,* 2002, **6**, 5.

[2] Mansoori, G. A., "Principles of Nanotechnology: Molecular Based Study of Condensed Matter in Small Systems", *World Sci. Pub. Co., Hackensack, NJ,* 2005.

[3] Plambeck, J. A., "Electroanalytical Chemistry: basic principles and applications", *Wiley (New York),* 1982, 302.

[4] Zhang, L., Teshima, N., Hasebe, T., Kurihara, M., Kawashima, T., *Talanta,* 1999, **50**, 677.

[5] Venton, B. J., *Analytical Chemistry,* 2003, **75**, 414.

[6] Wightman, R. M., May, L. J., Michael, A. C., *Analytical Chemistry,* 1988, **60**, 769A.

[7] Marttila, R. J., "Handbook of Parkinson's Disease", *W.C. Koller (Ed.),* 1987, 35.

[8] Pollay, Michael M.D., Roberts, P. A., *Neurosurgery,* 1980, **6**, 675.

[9] Rascol, O., Brooks, D. J., Korczyn, A. D., De Deyn, P. P., Clarke, C. E., Lang, A. E., *New England Journal of Medicine,* 2000, **342**, 1484.

[10] Combs, G. F., "The Vitamins: Fundamental Aspects in Nutrition and Health", *Academic press,* 1992, Chapter 9.

[11] Sternson, A. W., McCreery, R., Feinberg, B., Adams, R. N., *Journal of Electroanalytical Chemistry,* 1973, **46**, 313.

[12] Rueda, M., Aldaz, A., Sanchez-Burgos, F., *Electrochimica Acta,* 1978, **23**, 419.

[13] Tse, D. C., McCreery, R. L., Adams, R. N., *Journal of medicinal chemistry,* 1976, **19**, 37.

[14] Zhang, M., Gong, K., Zhang, H., Mao, L., *Biosensors and Bioelectronics,* 2005, **20**, 1270.

[15] Safavi, A., Maleki, N., Moradlou, O., Tajabadi, F., *Analytical biochemistry,* 2006, **359**, 224.

[16] Zheng, D., Ye, J., Zhou, L., Zhang, Y., Yu, C., *Journal of Electroanalytical Chemistry,* 2009, **625**, 82.

[17] Kim, Y. R., Bong, S., Kang. Y. J., Yang, Y., Mahajan, R. K., Kim, J. S., Kim, H., *Biosensors and Bioelectronics,* 2010, **25**, 2366.

[18] Nicholson, R. S., *Analytical Chemistry*, 1965, **37**, 1351.

[19] Vielstich, W., "Cyclic voltammetry", *John Wiley & Sons*, Ltd., 2010

[20] Wang, J., Li, M., Shi, Z., Li, N., Gu, Z., *Analytical Chemistry*, 2002, **74**, 1993.

[21] Zhang, M., Liu, K., Xiang, L., Lin, Y., Su, L., Mao, L., *Analytical Chemistry,* 2007, **79**, 6559.

[22] Profumo, A., Fagnoni, M., Merli, D., Quartarone, E., Protti, S., Dondi, D., Albini, A., *Analytical Chemistry*, 2006, **78**, 4194.

[23] Wu, L., Zhang, X., Ju, H., *Analytical Chemistry*, 2007, **79**, 4538.

[24] Zhou, M., Shang, L., Li, B., Huang, L., Dong, S., *Biosensors and Bioelectronics,* 2008, **24**, 442.

[25] Male, K. B., Hrapovic, S., Santini, J. M., Luong, J. H. T., *Analytical Chemistry,* 2007, **79**, 7831.

[26] Wang, J., Li, M., Shi, Z., Li, N., Gu, Z., *Analytical Chemistry,* 2002, **74**, 1993.

[27] Kachoosangi, R. T., Musameh, M. M., Abu-Yousef, I., Yousef, J. M., Kanan, S. M., Xiao, L., Davies, S. G., Russell, A., Compton, R. G., *Analytical Chemistry*, 2009, **81**, 435.

[28] Kang, X., Wang, J., Wu, H., Liu, J., Aksay, I. A., Lin, Y., *Talanta*, 2010, **81**, 754.

[29] Li, J., Guo, S., Zhai, Y., Wang, E., *Electrochemistry Communications*, 2009, **11**, 1085.

[30] Fang, Y., Guo, S., Zhu, C., Zhai, Y., Wang, E., *Langmuir*, 2010, **26**, 11277.

[31] Novoselov, K. S., Geim, A. K., Morozov, S. V., Jiang, D., Zhang, Y., Dubonos, S. V., Grigorieva, I. V., Firsov, A. A., *Science,* 2004, **306**, 666.

[32] A. K. Geim, K. S. Novoselov, *Nat. Mater.*, 2007, **6**, 183.

[33] Novoselov, K. S., Geim, A. K., Morozov, S. V., Jiang, D., Katsnelson, M. I., Grigorieva, I. V., Dubonos, S. V., Firsov, A. A., *Nature,* 2005, **438**, 197.

[34] Zhang, Y. B., Tan, Y. W., Stormer, H. L., Kim, P., *Nature,* 2005, **438**, 201.

[35] Lin, Y. M., Dimitrakopoulos, C., Jenkins, K. A., Farmer, D. B., Chiu, H. Y., Grill, A., Avouris, P., *Science*, 2010, **327**, 662.

[36] Tarascon, J. M., Armand, M., *Nature*, 2001, **414**, 359.

[37] Wang, Y., Li, Z., Wang, J., Li, J., & Lin, Y., *Trends in biotechnology*, 2011, **29**, 205.

[38] Kim, K. S., Zhao, Y., Jang, H., Lee, S. Y., Kim, J. M., Kim, K. S., Ahn, J. H., Kim, P., Choi, J. Y., Hong, B. H., *Nature*, 2009, **457**, 706.

[39] Xu, C., Wang, X., Zhu, J., *The Journal of Physical Chemistry C*, 2008, **112**, 19841.

[40] Zhou, M., Zhai, Y., Dong, S., *Analytical Chemistry*, 2009, **81**, 5603.

[41] Stankovich, S., Dikin, D. A., Dommett, G. H., Kohlhaas, K. M., Zimney, E. J., Stach, E. A., Ruoff, R. S., *Nature*, 2006, **442**, 282.

[42] Yu, A. P., Ramesh, P., Itkis, M. E., Bekyarova, E., Haddon, R. C. J., *The Journal of Physical Chemistry C,* 2007, **111**, 7565.

[43] Ao, Z. M., Yang, J., Li, S., Jiang, Q., *Chemical Physics Letters*, 2008, **461**, 276.

[44] Guo, S., Wang, E., *Nano Today*, 2011, **6**, 240.

[45] Kelly, K. L., Coronado, E., Zhao, L. L., Schatz, G. C., *The Journal of Physical Chemistry B*, 2003, **107**, 668.

[46] Narayanan, R., El-Sayed, M. A., *The Journal of Physical Chemistry B*, 2005, **109**, 12663.

[47] Hu, K., Lan, D., Li, X., Zhang, S., *Analytical Chemistry*, 2008, **80**, 9124.

[48] Liong, M., Lu, J., Kovochich, M., Xia, T., Ruehm, S. G., Nel, A. E., Zink, J. I., *Acs Nano*, 2008, **2**, 889.

[49] Jain, P. K., El-Sayed, I. H., El-Sayed, M. A., *Nano Today*, 2007, **2**, 18.

[50] Kasthuri, J., Veerapandian, S., Rajendiran, N., *Colloids and Surfaces B: Biointerfaces*, 2009, **68**, 55.

[51] Yu, A., Liang, Z., Cho, J., Caruso, F., *Nano letters*, 2003, **3**, 1203.

[52] Pingarrón, J. M., Yáñez-Sedeño, P., González-Cortés, A., *Electrochimica Acta*, 2008, **53**, 5848.

[53] Zhou, K., Zhu, Y., Yang, X., Luo, J., Li, C., Luan, S., *Electrochimica Acta*, 2010, **55**, 3055.

[54] Li, J., Liu, C. Y., Liu, Y., *Journal of Materials Chemistry*, 2012, **22**, 8426.

[55] Zhou, K., Zhu, Y., Yang, X., Li, C., *Electroanalysis*, 2010, **22**, 259.

[56] Hummers, W.S., Offeman, R.E., *Journal of the American Chemical Society,* 1958, **80**, 1339.

[57] Z.-L. Wang., D. Xu., Y. Huang., Z. Wu., L.-M. Wang., X. B. Zhang., *Chemical Communications*, 2012, **48**, 976.

[58] Chien, C. C., Jeng, K. T., *Materials chemistry and physics*, 2006, **99**, 80.

[59] Ago, H., Kugler, T., Cacialli, F., Salaneck, W. R., Shaffer, M. S., Windle, A. H., Friend, R. H., *The Journal of Physical Chemistry B*, 1999, **103**, 8116.

[60] Kong, B. S., Geng, J., Jung, H. T., *Chemical Communications*, 2009, **16**, 2174.

[61] Weast, R. C., *The American Journal of the Medical Sciences*, 1969, **257**, 423.

[62] Nalawade, P., Mukherjee, T., Kapoor, S., *Colloids and Surfaces A: Physicochemical and Engineering Aspects*, 2012, **396**, 336.

[63] Wang, S., Qian, K., Bi, X., Huang, W., *The Journal of Physical Chemistry C*, 2009, **113**, 6505.

[64] Moreau, F., Bond, G. C., Taylor, A. O., *Journal of Catalysis*, 2005, **231**, 105.

[65] Phonthammachai, N., White, T. J., *Langmuir*, 2007, **23**, 11421.

[66] Zhang, N., Qiu, H., Liu, Y., Wang, W., Li, Y., Wang, X., Gao, J., *Journal of Materials Chemistry*, 2011, **21**, 11080.

[67] Dong, X., Huang, W., Chen, P., *Nanoscale Research Letters*, 2011, **6**, 60.

[68] Li, Q., Wang, Y., Luo, G., *Materials Science and Engineering: C*, 2000, **11**, 71.

[69] Li, J., Yang, J., Yang, Z., Li, Y., Yu, S., Xu, Q., Hu, X., *Analytical Methods*, 2012, **4**, 1725.

요 약 (국문초록)

본 연구에서는 선택성과 민감도가 높은 도파민 바이오센서의 개발을 시도하였다. 도파민은 다양한 동물들의 중추 신경계에서 발견되는 신경 전달물질 (호르몬)로 분비되는 양에 따라 정신 분열증, 간질병, 파킨슨 병과 같은 질병과 깊은 연관이 있다. 따라서 고농도로 공존하는 아스코르빅산의 방해 없이 도파민을 정확하게 정량 검출하는 센서의 개발은 최근 많은 관심을 받고 있다. 본 실험에 사용된 그래핀은 Hummers의 방법으로 합성되었고 금의 전구체를 그래핀 위에서 곧바로 환원시켜서 그래핀/금 나노복합재를 합성하였다. 금 나노입자는 별도의 환원제나 capping agent 없이 수산화나트륨에 의해서 환원되었다. 수산화나트륨은 금 나노입자가 그래핀 표면 위에서 환원이 수월하게 이루어지게 하기 위한 촉진제로 사용되었으며 높은 재현성을 가진 합성법임을 증명하였다. 관련된 합성 메카니즘은 본문에서 자세히 논의되었다. 이후에 그래핀은 화학 및 열 처리과정을 거쳐서 환원되었다. 그래핀/금 나노복합재로 수식된 전극은 일반 그래핀으로 수식된 전극보다 훨씬 향상된 전기적 특성을 나타내었다. 합성된 그래핀/금 나노복합재는 X선 회절 분석 (XRD), X선 광전자 분광법 (XPS), 라만 분광법 (Raman spectroscopy), 열중량분석법 (TGA)을 이용하여 물리화학적 특성을 분석하였고 투과전자현미경 (TEM) 이미지를 이용하여 성공적으로 나노복합재가 합성되었음을 증명하였다. 수식된 전극의 전기적 특성은 완충용액에서 순환 전압전류법 (CV)과 시차펄스

전압전류법 (DPV)을 이용하여 분석하였다. 수식된 전극은 낮은 측정 한계치 (0.208 μM)를 나타내었다. 또한 일반 그래핀이 수식된 전극보다 아스코르빅산에서 도파민에 대해 전기화학적인 감응과 선택성이 증가하였음을 증명하였다.

주요어 : 그래핀/금 나노입자 복합 재료, 수산화나트륨, 바이오센서, 전압전류법, 도파민, 아스코르빅산

학 번 : 2011-23982